



Analytic and numeric solutions of moving boundary problems

M. Miklavčič

Department of Mathematics, Michigan State University, E. Lansing, MI 48824, United States of America



ARTICLE INFO

Article history:

Received 1 November 2020

Received in revised form 28 March 2023

Keywords:

Moving boundary problems

One-phase Stefan problem

Oxygen diffusion in absorbing media

Analytic solutions of moving boundary problems

ABSTRACT

A numerical method that gives accurate solutions of moving boundary problems that model diffusion of oxygen in a medium which consumes the oxygen is presented. The method is applied to the classic problem with a sealed surface as well as to problems with a permeable surface. Several new analytic solutions of moving boundary problems and of one-phase Stefan free boundary problems are presented and are used to study approximation errors of the numerical method.

© 2023 Elsevier B.V. All rights reserved.

1. Introduction

The problem of finding the region $0 < x < s(t)$ where the concentration $c(x, t)$ satisfies

$$\frac{\partial c}{\partial t} = \frac{\partial^2 c}{\partial x^2} - 1, \quad \text{for } 0 \leq x \leq s(t), \quad 0 \leq t \leq T \quad (1)$$

$$c(s(t), t) = 0, \quad \frac{\partial c}{\partial x}(s(t), t) = 0, \quad \text{for } 0 \leq t \leq T \quad (2)$$

$$\frac{\partial c}{\partial x}(0, t) = 0, \quad \text{for } 0 \leq t \leq T \quad (3)$$

$$c(x, 0) = \frac{1}{2}(1 - x)^2, \quad \text{for } 0 \leq x \leq 1, \quad s(0) = 1 \quad (4)$$

was introduced by Crank and Gupta [1] to model diffusion of oxygen in a medium which simultaneously consumes the oxygen. This is a classical moving boundary problem [2]. Its importance in the theory of free and moving boundary problems has been discussed by Ockendon in [3]. However, a great deal of uncertainty remained about accuracy of solutions. To illustrate the problem, consider the values, at an often quoted time $t = 0.16$, in Table 1.

The numerical method presented here is based on the fixed step, finite difference method. The essence of the method is in placement of the free boundary in the grid without destroying the structure of errors of the finite difference method. The main advantage of this method is highly predictable error, which can hence be mostly eliminated by Richardson extrapolation. Richardson extrapolation was actually used two times on this problem to match 21 significant digits of computed $s(t)$ with known asymptotic values at a small t .

Unlike the Fourier cosine series method used by Dahmardah and Mayers [10] or the integral method of Hansen and Hougaard [9], the numerical method presented here is not tied to (3), (4). Eq. (3) is indicating that the oxygen consuming region has a sealed surface at $x = 0$ and hence the region has to shrink. Replacing the sealed interface condition (3) with a prescribed concentration or a prescribed flux is, together with Eqs. (1), (2), a model of an oxygen consuming region with

E-mail address: milan@math.msu.edu.

Table 1
Some published approximations of $s(0.16)$.

$s(0.16)$	Authors
0.6710	Gupta and Banik [4], 1989
0.6784	Ahmed [5], 2006
0.6809	Gülkaç [6], 2009
0.68128	Crank and Gupta [1], 1972
0.68247	Gupta and Kumar [7], 1981
0.68317	Miller, Morton, Baines [8], 1978
0.68337	Hansen and Hougaard [9], 1974
0.683449	Dahmardah and Mayers [10], 1983

a permeable surface. In this case the region can expand or contract, depending on what is prescribed at $x = 0$, and thus the applicability of the model is greatly increased. In particular, it is shown here that the numerical method provides an accurate solution also when the supply of the oxygen at $x = 0$ is periodic.

Ignoring (3), (4), one can choose any smooth $s(t)$ and try to find $c(x, t)$ satisfying Eqs. (1), (2). This enabled us to find many analytic solutions of moving boundary problems and we used some of them to study approximation errors produced by our method. The detailed studies are included for the following selections of $s(t)$:

- 1: $s(t) = 2 - \cos(t)$ is used to test the numerical method's performance over long time when the region is contracting and expanding.
- 2: $s(t) = \sqrt{1 - 5t}$ is fairly similar to the solution of the original problem (1)–(4) and the analytic solution of Eqs. (1), (2) can be easily computed for this $s(t)$.
- 3: $s(t) = \sqrt{1 - 130t^3}$ is to the naked eye indistinguishable from the solution of (1)–(4), however, evaluation of the corresponding analytic solution is a bit more complex.

Availability of the analytic solutions was essential in choosing an appropriate formula for the location of the free boundary in the grid. Several candidates for the location were eliminated after producing large errors. Among them was the Crank and Gupta [1] choice.

The analytic solutions of the moving boundary problems appear to be new. The moving boundary problems are closely tied to the ancient Stefan free boundary problems which have very few known analytic solutions [11]. To see the connection, note that if c is a smooth solution of the moving boundary problem (1), (2) and if $u = c_t$ then obviously

$$\frac{\partial u}{\partial t} = \frac{\partial^2 u}{\partial x^2}, \quad \text{for } 0 \leq x \leq s(t), \quad 0 \leq t \leq T. \tag{5}$$

Differentiation of $c(s(t), t) = 0$ implies $u = 0$ and $c_{xx} = 1$ at $x = s(t)$. This and differentiation of $c_x(s(t), t) = 0$ imply

$$u(s(t), t) = 0, \quad \frac{\partial u}{\partial x}(s(t), t) = -s'(t), \quad \text{for } 0 \leq t \leq T. \tag{6}$$

(5), (6) is the standard part of one-phase Stefan free boundary problems. This connection between the problems was discussed by Ockendon in [3] and was observed earlier by Schatz [12]. Therefore, all analytic solutions presented in the next section are also analytic solutions of the Stefan free boundary problems after differentiation with respect to t . In particular, example 1 provides a simple periodic analytic solution of a one-phase Stefan free boundary problem.

2. Analytic solutions

As observed in [1], using Eqs. (1), (2) gives

$$c = 0, \quad \frac{\partial c}{\partial x} = 0, \quad \frac{\partial^2 c}{\partial x^2} = 1, \quad \frac{\partial^3 c}{\partial x^3} = -s', \quad \frac{\partial^4 c}{\partial x^4} = (s')^2 \dots \quad \text{at } x = s(t) \tag{7}$$

which implies that if c has 5 continuous derivatives in x we have to have

$$c(x, t) = \frac{(x - s(t))^2}{2} - \frac{(x - s(t))^3}{3!} s'(t) + \frac{(x - s(t))^4}{4!} s'(t)^2 + \int_{s(t)}^x \frac{(x - y)^4}{4!} \frac{\partial^5 c}{\partial x^5}(y, t) dy. \tag{8}$$

This will be used for our placement of the interface and it also suggests that for given arbitrary smooth $s(t)$ we look for the concentration $c(x, t)$ in the form

$$c(x, t) = \sum_{n=2}^{\infty} \frac{(x - s(t))^n}{n!} F_n(t). \tag{9}$$

Eqs. (1), (2) imply that F_n have to satisfy

$$F_2 = 1, \quad F_3 = -s' \tag{10}$$

$$F_n = -s' F_{n-1} + F'_{n-2}, \quad \text{for } n \geq 4. \tag{11}$$

In terms of these F_n , one can express solutions of the Stefan free boundary problem (5), (6) as

$$u(x, t) = \sum_{n=1}^{\infty} \frac{(x - s(t))^n}{n!} F_{n+2}(t). \tag{12}$$

For each $s(t)$ considered, we were able to reformulate (11) so that recursive integer computations quickly produced F_n for values of n far bigger than needed to achieve convergence in (9) or (12). Some examples are presented below.

In a special case when, for some constant α ,

$$s'' = \alpha(s')^3 \tag{13}$$

Eq. (11) implies that

$$F_n = a_n(s')^{n-2} \tag{14}$$

where

$$a_2 = 1, \quad a_3 = -1, \quad a_n = -a_{n-1} + \alpha(n - 4)a_{n-2} \quad \text{for } n \geq 4. \tag{15}$$

Using (14) in (9) enables us to rewrite $c(x, t)$ as

$$c(x, t) = \frac{1}{s'(t)^2} W((x - s(t))s'(t)), \quad \text{where } W(z) = \sum_{n=2}^{\infty} \frac{a_n z^n}{n!}. \tag{16}$$

Eq. (15) implies that the power series for W has infinite radius of convergence. It is easy to see that W can also be obtained as the solution of

$$W''(z) + (1 - \alpha z)W'(z) + 2\alpha W(z) = 1, \quad W(0) = W'(0) = 0. \tag{17}$$

Using $g(z) = 1 - \alpha - 2\alpha z + \alpha^2 z^2$ one can express W also as

$$W(z) = \int_0^z \int_0^u \frac{g(z)g(t)}{g(u)^2} e^{(u-t)((u+t)\alpha/2-1)} dt du.$$

If one chooses

$$s(t) = 1 - t/\tau \quad \text{with some } \tau \neq 0 \tag{18}$$

then (13) holds with $\alpha = 0$ and (16) can be rewritten as

$$c(x, t) = \tau^2 W(z) \quad \text{where } z = (1 - x - t/\tau)/\tau, \quad W(z) = e^{-z} - 1 + z \tag{19}$$

giving us an elementary analytic solution of (1), (2). This solution, for the corresponding Stefan problem, was found by Goodman [13].

If one chooses

$$s(t) = \sqrt{1 - t/\tau} \quad \text{with some } \tau \neq 0 \tag{20}$$

then (13) holds with $\alpha = 2\tau$. In this case (16) can be rewritten as

$$c(x, t) = \alpha^2 s(t)^2 W(z), \quad z = (1/\alpha)(1 - x/s(t)) \tag{21}$$

and is a solution of (1), (2). Note that flux at $x = 0$ is equal to

$$\frac{\partial c}{\partial x}(0, t) = c_1 \sqrt{\tau - t}, \quad \text{where } c_1 = -2\sqrt{\tau}W'(1/\alpha), \tag{22}$$

and the initial value is

$$c(x, 0) = \alpha^2 W((1 - x)/\alpha). \tag{23}$$

If one chooses

$$s(t) = \sqrt{1 - 130t^3} \tag{24}$$

then (13) does not hold, however, the graph of (24) is to the naked eye indistinguishable from the graph of $s(t)$ determined by the original problem (1)–(4). Eq. (11) suggests that we define

$$P_n(t) = F_n(t)s(t)^{n-2}. \tag{25}$$

P_n is a polynomial of degree $2(n - 2)$ given by

$$P_2 = 1, \quad P_3 = 195t^2, \quad P_n = 195t^2 P_{n-1} + (1 - 130t^3)P'_{n-2} + 195(n - 4)t^2 P_{n-2} \quad \text{for } n \geq 4. \tag{26}$$

In this case (9) can be rewritten as

$$c(x, t) = s(t)^2 \sum_{n=2}^{\infty} \left(\frac{x}{s(t)} - 1 \right)^n \frac{P_n(t)}{n!}. \tag{27}$$

It is a straightforward exercise to obtain the recursion relation for the integer coefficients of P_n which makes it possible to compute P_n fast and exactly.

To prove that (27) converges for every x when $0 < t < 130^{-1/3}$ define

$$Q_2 = P_2, \quad Q_3 = P_3, \quad Q_n = 195t^2Q_{n-1} + (1 + 130t^3)Q'_{n-2} + 195(n - 4)t^2Q_{n-2} \quad \text{for } n \geq 4. \tag{28}$$

Observe that, for each $n \geq 2$, Q_n is a polynomial of degree $2(n - 2)$ with nonnegative coefficients. This implies that $Q'_{n-2} \leq 2(n - 4)Q_{n-2}/t$ for $t > 0, n \geq 4$. Hence

$$Q_n \leq (2/t)(Q_{n-1} + 3(n - 4)Q_{n-2}) \quad \text{for } n \geq 4, \quad 0 < t < 130^{-1/3}. \tag{29}$$

By induction, the coefficients of Q_n are bigger or equal to the absolute values of the corresponding coefficients of P_n for $n \geq 2$ and therefore

$$|P_n(t)| \leq Q_n(t) \leq (2/t)^n \sqrt{n!} \quad \text{for } n \geq 4, \quad 0 < t < 130^{-1/3} \tag{30}$$

which proves that (27) defines an entire function of x for each $0 < t < 130^{-1/3}$.

Fig. 1 shows that the concentration c determined by (27) is fairly close to the concentration determined by the original problem (1)–(4).

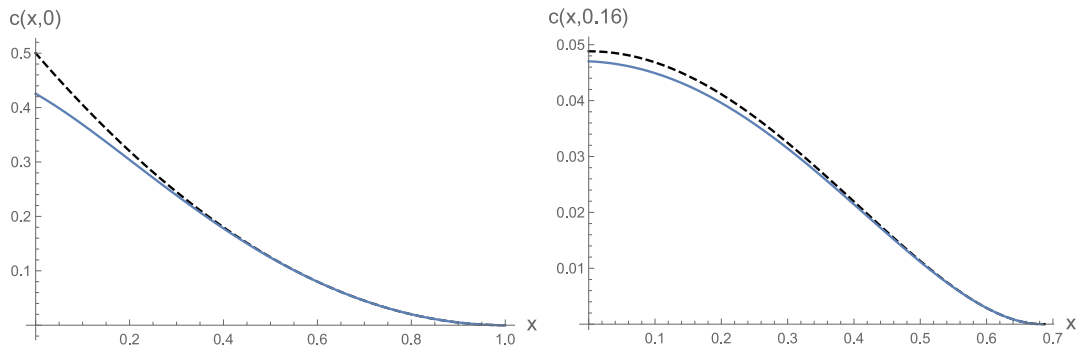


Fig. 1. Concentrations presented by the upper, dashed, curves satisfy (1)–(4). The lower curves are obtained from (27).

A good way to start studying the effect of a prescribed periodic concentration on a permeable surface is to study

$$s(t) = 2 - \cos(t). \tag{31}$$

Eq. (11) suggests that we write

$$F_n(t) = A_n(\sin(t)) + \cos(t)B_n(\sin(t)) \tag{32}$$

where $A_n(z)$ is a polynomial of degree $n - 2$ in z and $B_n(z)$ is a polynomial of degree $n - 5$. Set $B_n = 0$ for $n < 5$ and note that

$$A_2 = 1, \quad A_3 = -z, \quad A_n = -zA_{n-1} - zB_{n-2} + (1 - z^2)B'_{n-2} \quad \text{for } n \geq 4 \tag{33}$$

$$B_5 = -1, \quad B_n = -zB_{n-1} + A'_{n-2} \quad \text{for } n \geq 6. \tag{34}$$

For example,

$$A_9 = -z^7 + 25z^3 - 15z, \quad B_9 = -15z^4 + 1. \tag{35}$$

Again, it is a straightforward exercise to obtain the recursion relation for the integer coefficients of A_n and B_n which makes it possible to compute F_n fast and exactly.

The surface concentration $c(0, t)$ is graphed on Fig. 2 and it shows expected lag between when the maximum area is oxygenated and when the maximum concentration at the surface occurs. The derivative $c_t = u$ could also represent the temperature in water for $0 < x < s(t)$ bordering ice for $x > s(t)$ at the temperature 0. Note that the temperature at $x = 0$ turns negative at about $t = 2$, but the ice keeps melting a bit longer because of the presence of an insulating layer of water.

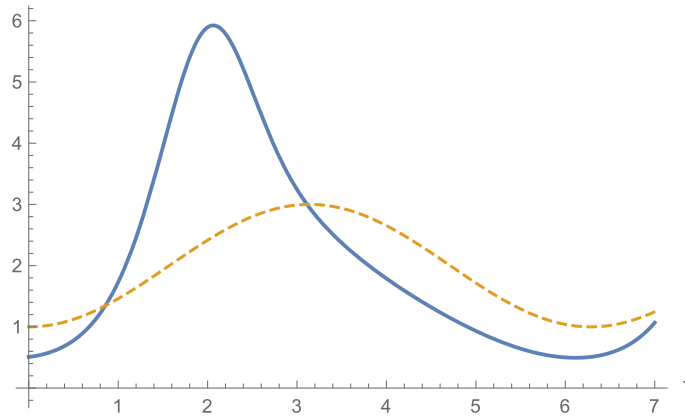


Fig. 2. Solid curve gives concentration $c(0, t)$ when $s(t) = 2 - \cos(t)$.

3. The numerical method

Let

$$x_i = (i - 1)h, \quad t_n = n\Delta t \quad i = 1, 2, \dots, r, r + 1, \quad n \geq 0 \tag{36}$$

$$c_i^n \approx c(x_i, t_n), \quad s_n \approx s(t_n), \quad s'_n \approx s'(t_n) \tag{37}$$

where h is a fixed space step size. The time step size Δt is chosen so that $\Delta t/h^2 \approx 0.4$ and that we finish at exactly the prescribed time.

We assume that initial values c_i^0 are given for $1 \leq i \leq r + 1$. The last grid point x_{r+1} should be always close to s_n , r may change with n . Initially the boundary is assumed to be at x_{r+1} , hence $s_0 = x_{r+1}$ and $c_{r+1}^0 = 0$.

We use the usual discretization of (1) to obtain concentrations at the next time level

$$\frac{c_i^{n+1} - c_i^n}{\Delta t} = \frac{c_{i-1}^n + c_{i+1}^n - 2c_i^n}{h^2} - 1 \quad \text{for } i = 2, \dots, r. \tag{38}$$

The condition on c at $x = 0$ determines c_1^{n+1} . See the note (a) below.

See the note (b) below for a derivation of

$$s'_{n+1} = \frac{y_1 - s_n + x_r}{\Delta t + y_1^2/6} \quad \text{where } y_1 = \sqrt{2c_r^{n+1}} \tag{39}$$

which we use to approximate the location of the free boundary at the next time level

$$s_{n+1} = s_n + s'_{n+1} \Delta t \quad \text{and let } y = s_{n+1} - x_r. \tag{40}$$

If $0.3h \leq y \leq 1.31h$ we do not change r and to complete the update we calculate

$$c_{r+1}^{n+1} = \frac{(y - h)^2}{2} + \frac{(y - h)^3}{6} s'_{n+1} + \frac{(y - h)^4}{24} (s'_{n+1})^2. \tag{41}$$

If $y < 0.3h$ we decrease r by 1 and for c_{r+1}^{n+1} we use the value already calculated.

If $y > 1.31h$ we first calculate c_{r+1}^{n+1} as in (41). Increase r by 1, decrease y by h and use (41) again.

This completes the update and gives all the details of our numerical method.

Here are some notes.

- (a) c_1^{n+1} is prescribed by the analytic solution in Examples 1 and 3. When the flux is prescribed at $x = 0$, one usually obtains c_1^{n+1} from (38) with $r = 1$ by defining

$$c_0^n = c_2^n - 2h \frac{\partial c}{\partial x}(0, t_n).$$

The flux is prescribed by the analytic solution in Example 2. Setting the flux to be 0, i.e. (3) is used, for the classical oxygen diffusion problem.

(b) Here is a derivation of (39). Note that (8) implies

$$\frac{y_1^2}{2} = c_r^{n+1} \approx c(x_r, t_{n+1}) = \frac{y^2}{2} + \frac{y^3}{6} s'(t_{n+1}) + \frac{y^4}{24} (s'(t_{n+1}))^2 + \dots \tag{42}$$

where $y = s(t_{n+1}) - x_r$. Hence

$$\frac{y_1^2}{y^2} \approx 1 + \frac{y s'(t_{n+1})}{3} + \frac{(y s'(t_{n+1}))^2}{12}. \tag{43}$$

Assuming that ys' is small gives

$$\frac{y}{y_1} \approx 1 - \frac{y s'_{n+1}}{6}, \tag{44}$$

$$y \approx y_1 - \frac{y_1^2 s'_{n+1}}{6}. \tag{45}$$

Using backward Euler approximation

$$y \approx s_n + s'_{n+1} \Delta t - x_r \tag{46}$$

with (45) gives s'_{n+1} in (39).

(c) Dropping $y_1^2/6$ in the denominator in (39) would change (40) to

$$s_{n+1} = y_1 + x_r. \tag{47}$$

This is the approximation of the position of the boundary that Crank and Gupta used (see (4.9) in [1]). Using the analytic solution in Example 2 below we show that this modification (47) drastically changes the approximation error.

(d) As expected, use of implicit trapezoidal method in place of backward Euler method in (46) does not change results. The same is true if $(ys')^2$ terms are kept in (44). This shows that the placement errors are small compared to the finite difference errors. The assumption that ys' is small implies the step size restriction

$$h|s'| \ll 1 \quad \text{i.e.} \quad \frac{|s'| \Delta t}{h} \ll \frac{\Delta t}{h^2} \tag{48}$$

This also explains why smaller step sizes are needed in Examples 2 and 3 than in Example 1 to achieve comparable accuracy.

(e) No grid point is added or removed when $s_{n+1} - x_r$ is in the interval $[0.3, 1.31]h$. We call that interval no r change window. The selections of $\Delta t/h^2 \approx 0.4$ and of the no r change window are rather arbitrary. Each example was recalculated at least 9 times with $\Delta t/h^2 \approx 0.4, 0.2, 0.45$ and windows $[0.3, 1.31]h, [0.5, 1.5]h, [0.6, 1.4]h$. Note that the third window is causing r to alternate, yet the final results do not change significantly.

More specifically, in Example 2, with $h = 1/320, \Delta t/h^2 = 0.4$ and window $[0.3, 1.31]h, r$ was reduced 177 times to reach $t = 0.16, r$ was unchanged 40783 times and it never increased. When the window changed to $[0.6, 1.4]h, r$ was reduced 4232 times, r was unchanged 32673 times and r increased 4055 times, however, the values of $c(0.2, 0.16)$ and $s(0.16)$ remained unchanged (up to the displayed accuracy). Using the window $[0, 1]h$ is not a good idea because (39) would require calculations of $\sqrt{2c_r^{n+1}}$ as $c_r^{n+1} \rightarrow 0$ and those values may become negative due to numerical errors. Change of $\Delta t/h^2$ changes the approximation error and a specific example is given in Table 7.

(f) At fixed (x, t) and fixed $\Delta t/h^2$, the approximation errors of both $c(x, t)$ and $s(t)$ are roughly proportional to h^2 . Richardson extrapolation (eliminating h^2 error terms) is shown to work very well in all cases. The second Richardson extrapolation (eliminating h^4 error terms) is shown to work well when solving the original problem using extended precision.

3.1. Example 1

We prescribe

$$s(t) = 2 - \cos(t), \quad 0 \leq t \leq 7$$

and evaluate analytic $c(x, t)$ that satisfies Eqs. (1), (2) as described at the end of Section 2. Let us call this analytic solution $Ac(x, t)$. Then we use our numerical method to solve (1), (2), with boundary condition (3) replaced by $c(0, t) = Ac(0, t)$ and with initial condition (4) replaced by $c(x, 0) = Ac(x, 0)$. The numerical method gives us the approximate $c(x, t)$ and the approximate $s(t)$.

Fig. 3 shows that s obtained by the numerical method traces the free boundary through expansion, contraction and new expansion. The concentration c obtained by the numerical method is even closer to the exact values as Fig. 4 shows.

Table 2 focuses on convergence at one point $x = 0.5, t = 7$. The error, the difference between the analytic solution and approximation, is denoted by ER. Note that the errors are (almost) proportional to h^2 and hence can be (almost) eliminated

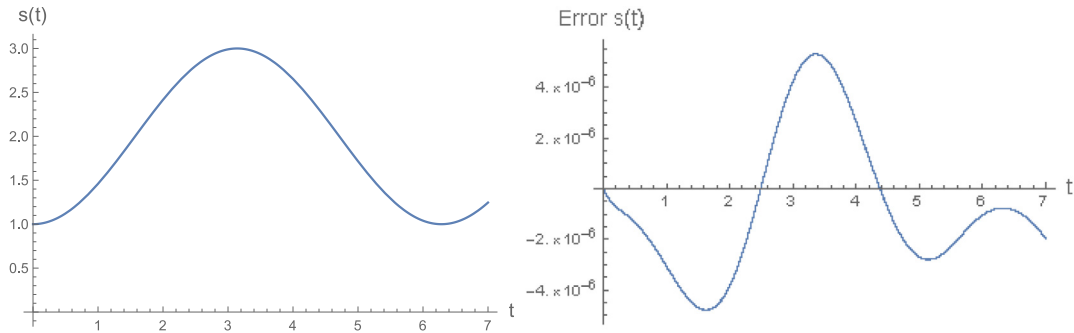


Fig. 3. $s(t) = 2 - \cos(t)$ on the left and on the right errors of numerical approximations of $s(t)$ when $h = 1/160$.

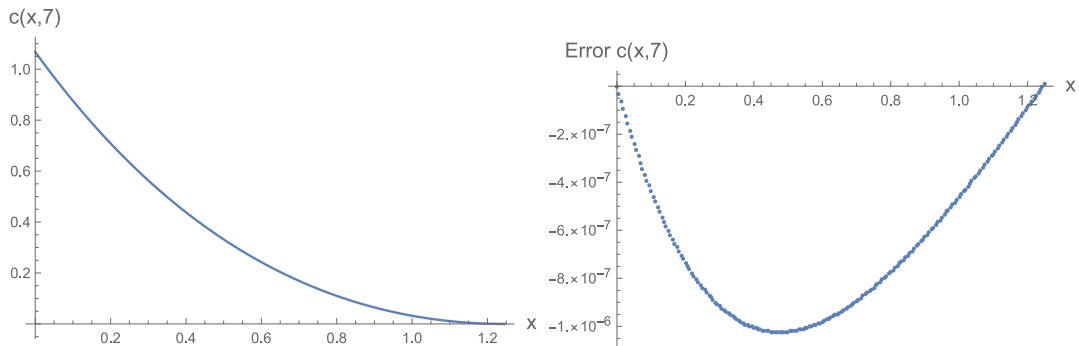


Fig. 4. Concentration $c(x, 7)$ on the left and on the right errors of numerical approximations of $c(x, 7)$ when $h = 1/160$.

the usual way (Richardson extrapolation). Note that approximate c is accurate to 5 digits in Table 2, but Richardson extrapolation gives 9 correct digits. Errors of s are a bit less predictable, and using Richardson extrapolation gives only three more correct digits.

Table 2

Approximations of $c(0.5, 7)$ and $s(7)$ depending on h when $s(t) = 2 - \cos(t)$. At $h = 0$ exact values are given. Rc is the Richardson extrapolation for c , ERc is the error of c , similarly for Rs , ERs .

h	$c(0.5, 7)$	Rc	ERc/h^2	$s(7)$	Rs	ERs/h^2
1/40	0.3318063127	0.3318226732	0.026176	1.246066234	1.246097418	0.0504
1/80	0.3318185826	0.3318226726	0.026176	1.246089837	1.246097704	0.0506
1/160	0.3318216501	0.3318226725	0.026177	1.246095763	1.246097739	0.0507
0	0.3318226726			1.246097746		

3.2. Example 2

We prescribe

$$s(t) = \sqrt{1 - 5t}, \quad 0 \leq t \leq 0.2$$

like in (20) with $\tau = 0.2$. We find W determined by the ODE (17) with $\alpha = 0.4$ (and in (22) $c_1 = -0.64\dots$) and then we use our numerical method to approximate $c(x, t)$ and $s(t)$ that are determined by the moving boundary problem (1), (2), (22), (23).

This example is much closer to the original problem (1)–(4) and has a simple analytic solution (21). Fig. 5 show how well the numerical method recovers $s(t)$. Concentrations are approximated even better as Fig. 6 shows.

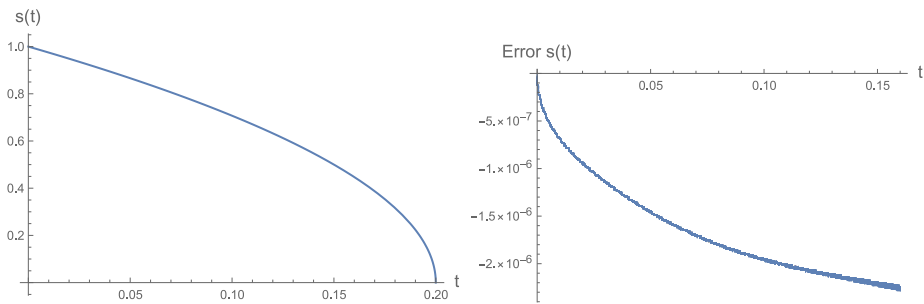


Fig. 5. $s(t) = \sqrt{1 - 5t}$ on the left and on the right errors of numerical approximations of $s(t)$ when $h = 1/320$.

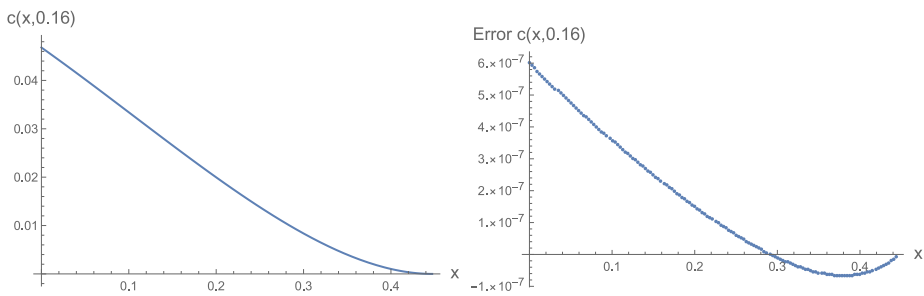


Fig. 6. Concentration at $t = 0.16$ on the left, $s(t) = \sqrt{1 - 5t}$. Approximation errors on the right when $h = 1/320$.

The essential part of our numerical method is the placement of the interface in the grid (39), (40). To see what happens with the approximation errors when our placement is replaced with (47), which was used by Crank and Gupta [1], consider Fig. 7 and compare it to Fig. 5.

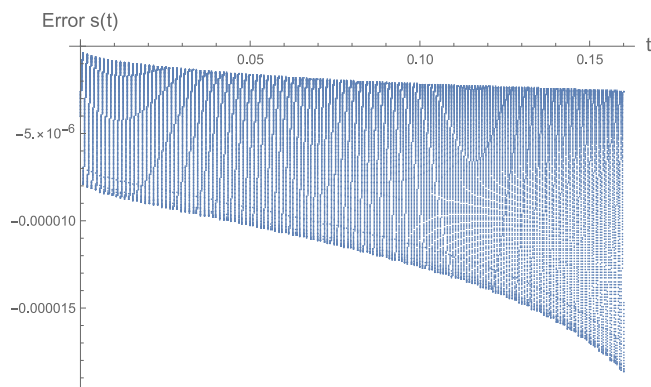


Fig. 7. Errors of numerical approximations of $s(t)$, $h = 1/320$, when a Crank and Gupta [1] position placement (47) is used.

Table 3 focuses on errors at the point $x = 0.2$, $t = 0.16$. As expected, Richardson extrapolation significantly improves accuracy.

Table 3

Approximations of $c(0.2, 0.16)$ and $s(0.16)$ depending on h when $s(t) = \sqrt{1 - 5t}$. At $h = 0$ exact values are given. Rc is the Richardson extrapolation for c , ERc is the error of c , similarly for Rs, ERs.

h	$c(0.2, 0.16)$	Rc	ERc/ h^2	$s(0.16)$	Rs	ERs/ h^2
1/80	0.0199679650	0.0199655739	-0.015342	0.44717888	0.44721131	0.2222
1/160	0.0199661674	0.0199655682	-0.015349	0.44720459	0.44721316	0.2304
1/320	0.0199657177	0.0199655678	-0.015351	0.44721136	0.44721361	0.2290
0	0.0199655678			0.44721360		

3.3. Example 3

We prescribe

$$s(t) = \sqrt{1 - 130t^3}$$

and use (27) to evaluate analytic $c(x, t)$ that satisfies Eqs. (1), (2). Let us call this analytic solution $Ac(x, t)$. Then we use our numerical method to solve (1), (2), with boundary condition (3) replaced by $c(0, t) = Ac(0, t)$ and with initial condition (4) replaced by $c(x, 0) = Ac(x, 0)$. The numerical method gives us the approximate $c(x, t)$ and the approximate $s(t)$.

Fig. 8 shows how the approximate $s(t)$ obtained by the numerical method compares to the exact solution. Concentrations are approximated even better as Fig. 9 shows.

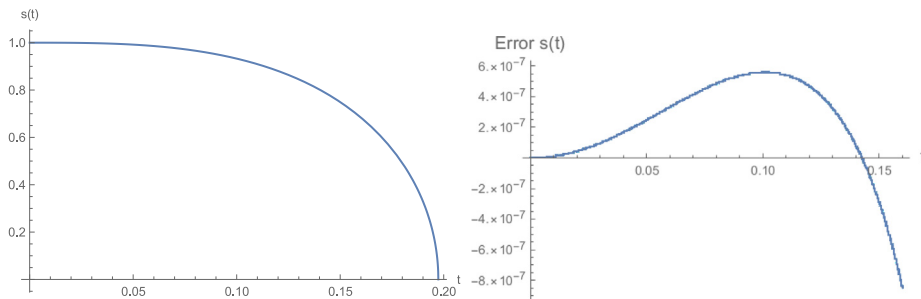


Fig. 8. $s(t) = \sqrt{1 - 130t^3}$ on the left and on the right errors of numerical approximations of $s(t)$ when $h = 1/640$.

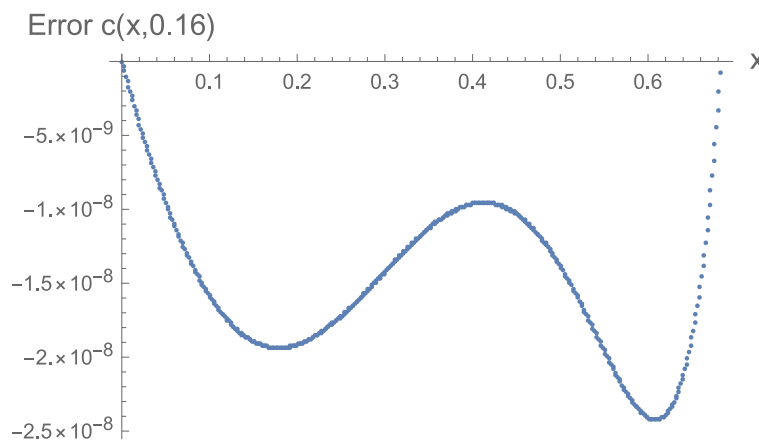


Fig. 9. Approximation errors of $c(x, 0.16)$ when $s(t) = \sqrt{1 - 130t^3}$ and $h = 1/640$. See Fig. 1 for $c(x, 0.16)$.

Table 4 focuses on errors at the point $x = 0.2, t = 0.16$. As expected, Richardson extrapolation improves accuracy. To estimate the size of the approximation error of $s(0.16)$, without knowing the exact value, consider the variation of $ERs/h^2 \approx 0.0033$. This suggests uncertainty of the approximation $s(0.16)$ to be $0.0033h^2 \approx 8 \times 10^{-8}$, which is exactly correct as a comparison to the exact solution shows. One can use Richardson extrapolation, in place of the exact solution, to estimate ERs and if this is done with data in the Table 4 the uncertainty would be estimated to be 2×10^{-8} .

Table 4

Approximations of $c(0.2, 0.16)$ and $s(0.16)$ depending on h when $s(t) = \sqrt{1 - 130t^3}$. At $h = 0$ exact values are given. Rc is the Richardson extrapolation for c , ERc is the error of c , similarly for Rs, ERs.

h	$c(0.2, 0.16)$	Rc	ERc/h^2	$s(0.16)$	Rs	ERs/h^2
1/80	0.03958315767	0.03958437764	0.007838	0.68370193	0.68375790	0.3355
1/160	0.03958407593	0.03958438202	0.007843	0.68374065	0.68375355	0.3506
1/320	0.03958430571	0.03958438230	0.007845	0.68375098	0.68375442	0.3445
1/640	0.03958436316	0.03958438231	0.007845	0.68375349	0.68375433	0.3478
0	0.03958438232			0.68375434		

4. The classical problem

When applying the numerical method to the classical problem (1)–(4) the errors behave the same way as in previous examples. To illustrate this at one point consider Table 5 and note similarity to Tables 2, 3, 4 where the analytic solution is known. Note also how close the values of $s(0.16)$ in Table 4 are to those in Table 5.

Table 5

Approximations of $c(0, 0.16)$ and $s(0.16)$ depending on h for the classical problem. Rc is the Richardson extrapolation for c , ERc is the error estimate of c and similarly for Rs and ERS . $\Delta t/h^2 = 0.4$, no r change window $[0.3, 1.31]h$ as in Tables 2, 3, 4.

h	$c(0, 0.16)$	Rc	ERc/h^2	$s(0.16)$	Rs	ERS/h^2
1/80	0.04882717112	0.04882274000	-0.028359	0.68343510	0.68345694	0.1398
1/160	0.04882384648	0.04882273826	-0.028370	0.68344540	0.68344883	0.0879
1/320	0.04882301524	0.04882273815	-0.028373	0.68344869	0.68344979	0.1124
1/640	0.04882280742	0.04882273815	-0.028374	0.68344943	0.68344967	0.1003

For the error estimate we use the difference between the Richardson extrapolation and the approximate value, which is the same as $1/3$ of the difference between successive approximations. Just like in the previous examples, the error estimates are almost proportional to h^2 which supports the use of the Richardson extrapolation.

Observe that the variations of ERS/h^2 in Table 5 suggests uncertainty $0.01h^2 \approx 2 \times 10^{-8}$ of Rs , the Richardson extrapolation for $s(0.16)$, i.e. the last two digits of the correct $s(0.16)$ should be between 65 and 69. To get good results near the extinction time we needed to decrease step size because of (48) and those calculations made it clear that the last two digits should be 68.3, i.e. $s(0.16) = 0.683449683$. Richardson extrapolations of $c(0, 0.16)$ in Table 5 converged, so we assume they converged to the correct $c(0, 0.16)$ as they did in Tables 2, 3, 4. Looking at the effect of variations ERc/h^2 confirms this as do calculations with smaller step sizes.

Each reference value in Table 6 is a product of an analysis like above. At small times and small step sizes second Richardson extrapolation was used and is described in the next section. To get higher accuracy one simply needs to decrease the step size (and perhaps increase calculation precision).

The values of $s(t)$, $0 \leq t \leq 0.1974$, are plotted in Fig. 10 along with the values of $c(x, 0.1974)$. The graph of $c(x, 0.16)$ is given in Fig. 1.

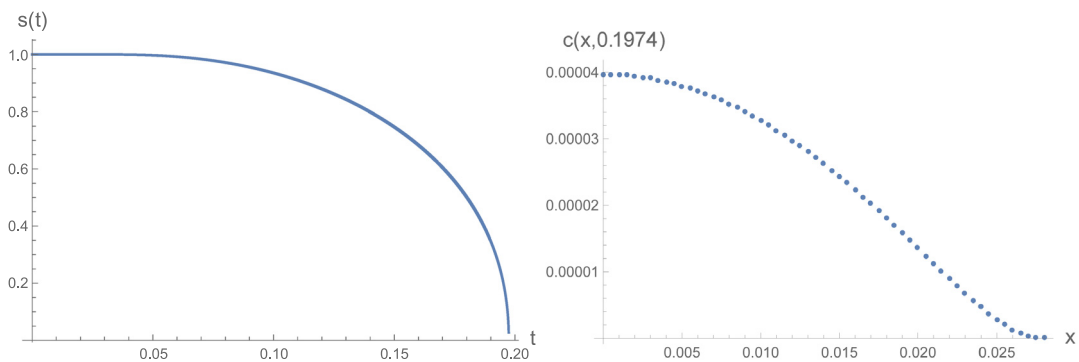


Fig. 10. $s(t)$ for $0 \leq t \leq 0.1974$ on the left. On the right $c(x, 0.1974)$ using $h = 0.0005$.

Note that in Table 1 the estimate by Dahmardah and Mayers [10] stands out. Accuracy in subsequent publications is significantly lower and in some more recent ones, like [5,6,14,15], there is not even a mention of [10].

Looking closer at other values obtained by Dahmardah and Mayers we see that they all agree with values given in Table 6 except for $s(t)$ at the following times. At $t = 0.1, 0.16, 0.18, 0.19$ the last digit of $s(t)$ in [10] is incorrect and at $t = 0.1974$ the last two digits are not correct. They [10] do mention that they change their method for $t > 0.19$. Table 6 gives roughly three times as many correct significant digits for $c(0, t)$ as [10].

The agreement between Dahmardah and Mayers [10] values and our values strongly validates both methods since the methods are totally different. Here are some advantages of our method:

- The boundary condition (3) is essential for Dahmardah and Mayers [10]. It is shown that our method produces accurate results also when $c(0, t)$ or $c_x(0, t)$ is prescribed.
- Our method is far simpler, it uses the standard finite difference method with a good formula for placement of the interface.

The extinction time appears to be 0.19743499. This is based on the behavior of $c(x, t)$ and $s(t)$ as shown in Figs. 11, 12 that were obtained by using our numerical method with $h = 1/8000$ and 30 digits precision. Using the four times larger step-size increases the estimate only by 1×10^{-8} .

Table 6
Solution of (1)–(4).

t	$c(0, t)$	$s(t)$
0.01	0.38716208329044874	0.99999999996925080411
0.02	0.34042308783942693	0.99999885336981993
0.03	0.304558995238832050	0.99991078825844
0.04	0.274324166581016006	0.999179863682
0.05	0.2476867478222685186	0.996792863038
0.06	0.2236046813091930066	0.99180215099
0.07	0.2014589459431846656	0.98353874647
0.08	0.1808462632897706421	0.97155001835
0.09	0.1614866723976611653	0.9554876666
0.10	0.14317670355494983665	0.9350171608
0.11	0.1257634448253636480	0.9097481959
0.12	0.1091292263919269625	0.8791705433
0.13	0.093182165146348042	0.8425765432
0.14	0.077850211527254121	0.7989438994
0.15	0.063077525494294867	0.746728768
0.16	0.048822738147725998	0.683449683
0.17	0.035059423244806462	0.604712309
0.18	0.02178093410019438	0.501330379
0.19	0.0090208775991420	0.346001505
0.1974	0.0000397192000	0.027829

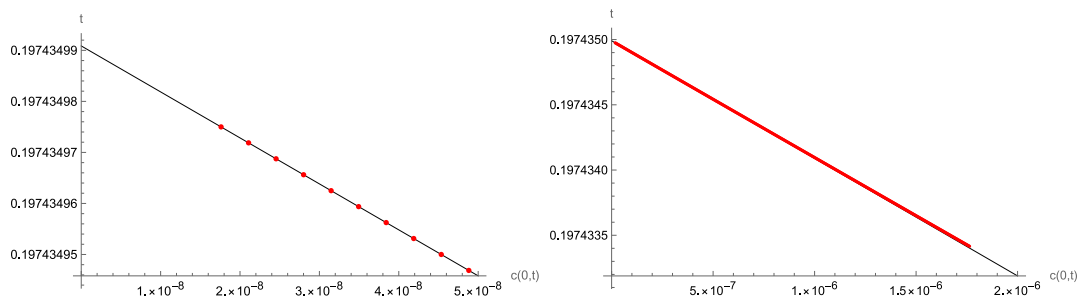


Fig. 11. The line on the left is fitted to the last 10 points of $c(0, t)$ that we calculated. The graph on the right shows the same line with the last 500 points.

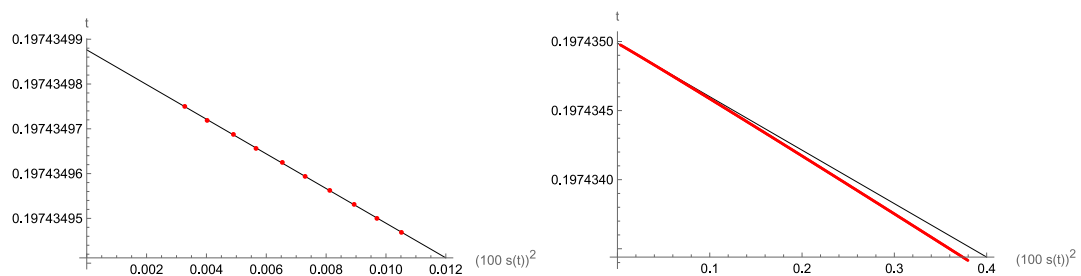


Fig. 12. The line on the left is fitted to the last 10 points of $s(t)$ that we calculated. The graph on the right shows the same line with the last 500 points.

5. Small time solution for the classical problem

A concern was expressed [1] that numerical methods based on finite difference methods are liable to give inaccurate solutions in the neighborhood of the surface for short times due to discontinuity of the gradient of the imposed initial concentration. The following comparison of our results to asymptotic behavior of the solution for short times shows that this concern is not justified. Furthermore, the 21 digit agreement with known asymptotic values provides another confirmation of the numerical method presented here.

Crank and Gupta [1] provide approximation

$$c(0, t) \approx \frac{1}{2} - 2\sqrt{\frac{t}{\pi}} \quad \text{for small } t. \tag{49}$$

They also observed that integration of (1) implies

$$s(t) = - \int_0^{s(t)} \frac{\partial c}{\partial t}(x, t) dx$$

which, together with their Laplace approximation of $c(x, t)$ (all $n = 0$ terms), implies

$$s(t) \approx \frac{1}{\sqrt{\pi t}} \int_0^{s(t)} \left(e^{-\frac{x^2}{4t}} - e^{-\frac{(2-x)^2}{4t}} \right) dx \quad \text{for small } t$$

and this simplifies [9] to

$$s(t) \approx 2 \operatorname{erf}\left(\frac{1}{\sqrt{4t}}\right) - 1 \quad \text{for small } t. \tag{50}$$

Since $s(0.01)$ is very close to 1 we did calculations with 25 (and more) digits of precision instead of the usual 16 digits. Table 7 presents the same kind of a portrait of convergence at a particular point as do the above Tables 2, 3, 4, 5. However, due to extended precision calculations we can extract more info from Table 7 by using the second Richardson extrapolation to eliminate h^4 terms in the error as follows

$$ER2_h = \frac{R_h - R_{2h}}{15}, \quad R2_h = R_h + ER2_h.$$

This is done for c and for s in Table 8.

Table 7

a stands for 0.387162 and b stands for 0.99999999999692. Same labels as in Table 5. In the last row, $c(0, 0.01)$ is calculated by (49) and $s(0.01)$ is obtained from (50). The last two rows were used to obtain ER values in the last row. Calculations were done with Mathematica \$MinPrecision = 25, \Delta t/h^2 = 0.2. ERc is 3 times smaller and ERs is about 6 times larger when $\Delta t/h^2 = 0.4$.

h	$c(0, 0.01)$	Rc	ERc/ h^2	$s(0.01)$	Rs	ERs/ h^2
0.001	a50643360612	a08328656958	-0.4231470	b8800269	b5088289	-3.712×10^{-9}
0.0005	a18907605626	a08329020631	-0.4231434	b6010745	b5080904	-3.719×10^{-9}
0.00025	a10973683926	a08329043359	-0.4231425	b5313018	b5080442	-3.721×10^{-9}
	a08329044874		-0.4231422	b5080411		-3.722×10^{-9}

Table 8

The second Richardson extrapolation (R2) applied to Rc and Rs values in Table 7.

h	Rc	R2c	ER2c/ h^4	Rs	R2s	ER2s/ h^4
0.001	a08328656958			b5088289		
0.0005	a08329020631	a08329044876	3.8792	b5080904	b5080412	-7.88×10^{-6}
0.00025	a08329043359	a08329044874	3.8789	b5080442	b5080411	-7.89×10^{-6}

The values at $t = 0.01$ in Table 6 are obtained from Table 8. Note that variation of $ER2s/h^4$ suggests uncertainty of R2s to be $10^{-8}h^4 \approx 4 \times 10^{-23}$, so, the last displayed digit of $s(0.01)$ should be correct. Same for $c(0, 0.01)$. Note that all 21 digits for $s(0.01)$ and all 17 digits for $c(0, 0.01)$ are equal to asymptotic values given by (49), (50). This shows that our method works very well also for short times when solving the classical oxygen diffusion problem in an absorbing media with a sealed interface.

At $t = 0.02$ our value of the concentration still agrees with (49) but our 11th digit of s differs from the asymptotic value given by (50). At $t = 0.03$ the 17th digit of our value of the concentration differs from (49) and our 9th digit of s differs from the asymptotic value given by (50).

6. Conclusions

For many smooth $s(t)$ we obtained analytic solutions of the moving boundary problem (1), (2) and some examples are presented in Section 2. These solutions are also solutions of the Stefan problem (5), (6) after differentiation with respect to t .

These solutions can be used to test numerical methods developed for moving boundary problems and Stefan problems. By applying the numerical method presented here for solving moving boundary problems to problems with known analytic solutions we demonstrated that our numerical method provides accurate solutions with very predictable approximation error.

By applying the numerical method to the classical oxygen diffusion problem in an absorbing media with a sealed interface we obtained a solution that is significantly more accurate than other published solutions.

The numerical method can be easily applied also when the interface is not sealed at $x = 0$. In particular, it was shown that it provides an accurate solution also when the interface is permeable and the supply of oxygen is periodic.

Data availability

Data will be made available on request.

References

- [1] J. Crank, R.S. Gupta, A moving boundary problem arising from the diffusion of oxygen in absorbing tissue, *J. Inst. Math. Appl.* 10 (1972) 19–33.
- [2] J. Crank, *Free and Moving Boundary Problems*, Clarendon Press, Oxford, 1984.
- [3] J.R. Ockendon, The role of the Crank-Gupta model in the theory of free and moving boundary problems, *Adv. Comput. Math.* 6 (1996) 281–293.
- [4] R.S. Gupta, N.C. Banik, Approximate method for the oxygen diffusion problem, *Int. J. Heat Mass Transfer* 32 (1989) 781–783.
- [5] S.G. Ahmed, A numerical method for oxygen diffusion and absorption in a sike cell, *Appl. Math. Comput.* 173 (2006) 668–682.
- [6] V. Gülkaç, Comparative study between two numerical methods for oxygen diffusion problem, *Commun. Numer. Methods. Eng.* 25 (2009) 855–863.
- [7] R.S. Gupta, D. Kumar, Complete numerical solution of the oxygen diffusion problem involving a moving boundary, *Comput. Methods Appl. Mech. Engrg.* 29 (1981) 233–239.
- [8] J.V. Miller, K.W. Morton, M.J. Baines, A finite element moving boundary computation with an adaptive mesh, *J. Inst. Math. Appl.* 22 (1978) 467–477.
- [9] E. Hansen, P. Hougaard, On a moving boundary problem from biomechanics, *J. Inst. Math. Appl.* 13 (1974) 385–398.
- [10] H.O. Dahmardah, D.F. Mayers, A Fourier-series solution of the Crank-Gupta equation, *IMA J. Numer. Anal.* 3 (1983) 81–85.
- [11] M. Mamode, Quasi similarity solutions for one phase stephan problems with time-dependent boundary conditions, *SIAM J Appl Math* 74 (2014) 1036–1057.
- [12] J. Schatz, Free boundary problems of stephan type with prescribed flux, *J. Math. Anal. Appl.* 28 (1969) 569–580.
- [13] T.R. Goodman, The heat-balance integral and its application to problems involving a change of phase, *Trans. ASME* 80 (1958) 335–342.
- [14] A. Bouregghda, Numerical solution of the oxygen diffusion in absorbing tissue with a moving boundary, *Commun. Numer. Methods. Eng.* 22 (2006) 933–942.
- [15] S.L. Mitchell, An accurate application of the integral method applied to the diffusion of oxygen in absorbing tissue, *Appl. Math. Model.* 38 (2014) 4396–4408.